Field emission of electrons from hemispherical conducting Carbon Nanotube tip

A Dissertation submitted towards the partial fulfillment of
the requirement for the award of degree of

Master of Technology
in
Nano Science and Technology

Submitted by

Suresh Kumar Mahan
2K13/NST/14

Under the supervision of

Prof. S.C. Sharma
(HOD, Applied Physics)

Department of Applied Physics

Delhi Technological University
(Formerly Delhi College of Engineering)
Delhi-110042
JUNE 2015

DELHI TECHNOLOGICAL UNIVERSITY
Established by Govt. Of Delhi vide Act 6 of 2009
(Formerly Delhi College of Engineering)
SHAHBAD DAULATPUR, BAWANA ROAD, DELHI-110042

CERTIFICATE

This is to certify that work which is being presented in the dissertation entitled **Field emission of electrons from hemispherical conducting Carbon Nanotube tip** is the authentic work of **Suresh Kumar Mahan** under my guidance and supervision in the partial fulfillment of requirement towards the degree of **Master of Technology in Nano Science and Technology**, run by Department of Applied Physics in Delhi Technological University during the year 2013-2015.

As per the candidate declaration this work has not been submitted elsewhere for the award of any other degree.

Prof. S. C. Sharma

Supervisor

H.O.D., Applied Physics

Delhi Technological University,

Delhi

DECLARATION

I hereby declare that all the information in this document has been obtained and presented in accordance with academic rules and ethical conduct. This report is my own, unaided work. I have fully cited and referenced all material and results that are not original to this work. It is being submitted for the degree of Master of Technology in Engineering at the Delhi Technological University. It has not been submitted before for any degree or examination in any other university.

Signature :

Name : Suresh Kumar Mahan

ACKNOWLEDGEMENT

I take this opportunity as a privilege to thank all individuals without whose support and guidance I could not have completed my project successfully in this stipulated period of time.

First and foremost I would like to express my deepest gratitude to my supervisor **Prof. S.C. Sharma**, HOD, Applied Physics, for his invaluable support, guidance, motivation and encouragement throughout the period this work was carried out.

I am also thankful to **Ms Aarti Tewari** and **Mr. Ravi Gupta (Research scholars)** for their valuable support and guidance in carrying out this project.

I am deeply grateful to **Dr. Pawan Kumar Tyagi** (Branch coordinator, NST) for his support and encouragement in carrying out this project.

I also wish to express my heart full thanks to **Mr. Anand Sharma** (classmate) as well as staff at Department of Applied Physics of Delhi Technological University for their goodwill and support that helped me a lot in successful completion of this project.

.

Suresh Kumar Mahan
M. Tech. (NST)
2K13/NST/14

ABSTRACT

The present work examines the field emission from conducting hemispherical Carbon Nanotune (CNT) tip. An expression for electrostatic potential for a hemispherical CNT tip at a distance from the centre of CNT has been derived. Using the time-independent Schrodinger equation corresponding expressions for transmission coefficient and field emission current density have been derived for the hemispherical conducting carbon nanotubes. The numerical calculations of potential, transmission coefficient and the current density function have been calculated for a typical set of carbon nanotube parameters. From the expression of potential energy we found that the potential energy for the hemispherical CNT tip decreases with the radial distance. The transmission coefficient increases with the normalized radial energy. And the current density function also increases with the normalized fermi energy. An important outcome of the present work is that both transmission coefficient and field emission current density function decreases as the hemispherical CNT tip radius increases.

.

TABLE OF CONTENTS

CHAPTERS

LIST OF FIGURES

LIST OF TABLES

LIST OF SYMBOLS

E	Electric field
V(r)	Potential energy
σ	Surface Charge density
r	Distance from the centre of hemispherical CNT
h	Distance from the surface of hemispherical CNT
a	Radius of hemispherical CNT
m_e	Mass of electron
ε_0	Permittivity in free space
β	Field enhancement factor
q	Electric charge
$\hbar$	Planck's constant
ψ	Wave function
ε_ρ	Normalized radial energy
ε_f	Fermi energy
$T(\varepsilon_\rho)$	Electron transmission probability
J	Field emission current density
ϕ	Current density function

Chapter 1

CARBON NANOTUBES

1.1 Discovery of Carbon Nanotubes

Carbon is a very interesting element which has plays a very important role in our living or non living world. Carbon is present in various forms in 0-D, 1-D, 2-D and 3-D materials, 0-D such as small clusters and fullerenes, 1-D as carbon nanotube, 2-D as graphene and graphane and 3-D as nano diamonds. Carbon is being shaped not only in soccer molecules but also in cylindrical tubes. Carbon atoms can be used to build long cylindrical tubes and these were called buckytubes and in present time they are called as carbon nanotube, in short CNT.

1.2 Carbon Nanotubes (CNTs)

The 1-D form of carbon was observed under a transmission electron microscope. Carbon nanotubes can be defined as cylinders which are made of graphite sheets with closed at the ends. So the carbon nanotubes can consider as folding of a graphite sheet, just as one roll of a piece of paper into a cylinder form.

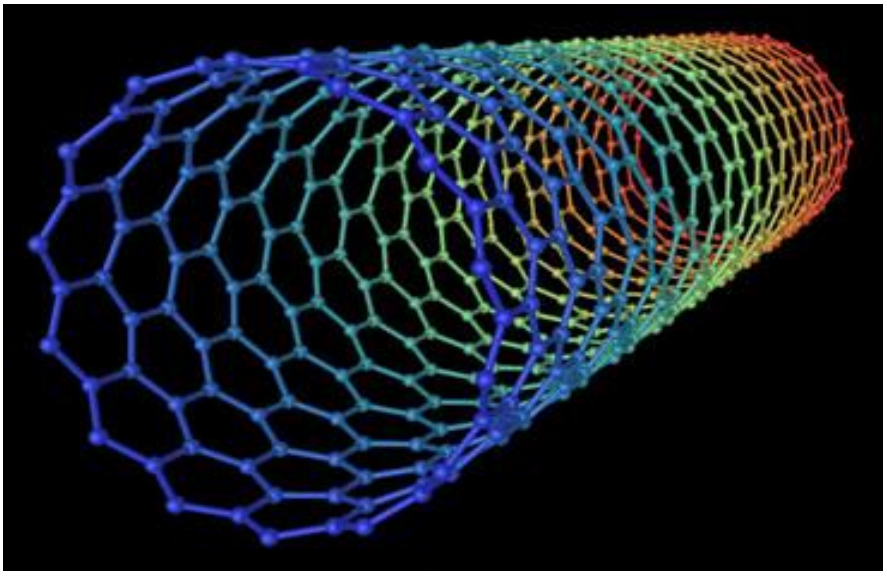

Fig. 1.1 Structure of Carbon Nanotube

In graphite sheet, the carbon atoms are spread in hexagonal arrangement. If there are many concentric cylinders which form a nanotube, are known as Multi Walled Carbon Nanotubes (MWCNTs). The distance between of MWCNT wall is around 0.334 nm. These MWCNTs are most common and are easily formed. In some conditions, there is a single folding of graphite, which is known as Single Wall Carbon Nanotubes (SWCNTs). By using some etching methods, MWCNTs can be turned into SWCNTs.

1.3 Structure of Carbon Nanotubes

In ideal case, we can consider a graphene sheet (graphene is a poly aromatic mono atomic layer which consists sp^2-hybridized carbon atoms that are formatted in hexagons) and it is to be rolled into a cylinder, in such a way that the hexagonal rings are localized in contact with each other. Then two caps that are hemispherical of the suitable diameter are varnished at both ends of the nanotube.

1.3.1 Single-Walled Nanotubes (SWNT)

Single Walled Nanotubes are defined as tubes of rolled graphite sheet in which the tubes are capped at both the ends with hemispherical structure. The structure of the SWNT could be imagined a layer of graphite sheet in which the graphite sheet is rolled into a cylinder.

SWNT have unique mechanical and electronic properties which can be used in so many applications like field emission displays, logic elements, nano composite materials and nano sensors.

In some Single Walled Nanotubes diameter is 0.4 nm and these nanotubes have been successfully synthesized. The length of the tube is very longer.

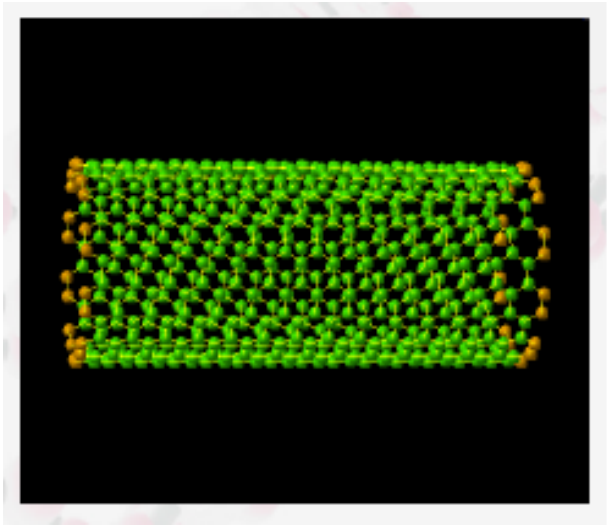

Fig. 1.2 Single-Walled Nanotube

1.3.2 Multi-Walled Nanotubes (MWNTs)

These are nanotubes that can be in the form of a coaxial arrangement of SWNT which is similar to a coaxial pipe of different radius. The inner diameter of the multi walled nanotube is generally in the range of 1.5 nm to 15 nm and the outer diameter of the MWNT is in the range of 2.5 nm to 50 nm. MWNT can be easily produced when it is in high volume quantities than SWNT. MWNT has a greater complex structure so the structure of this tube is not easliy understood. SWNTs have a better performance than MWNTs.

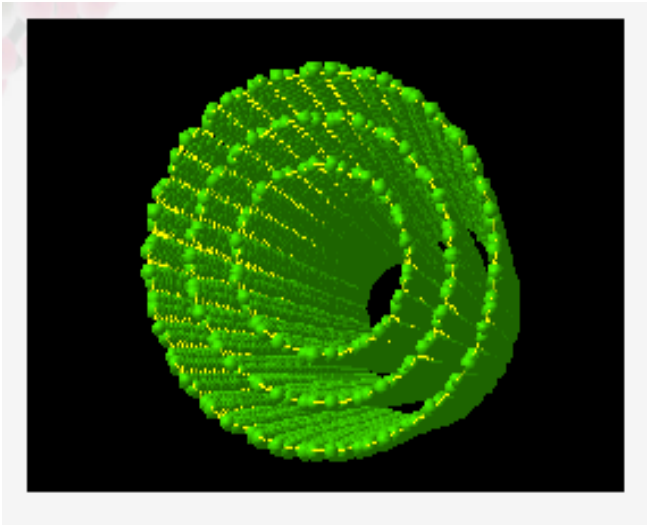

Fig. 1.3 Multi-Walled Nanotube

1.4 Nanotube Geometry

There are many ways in which we can roll a graphene sheet into a single-walled nanotube. There is plane of symmetry in parallel as well as in perpendicular ways with the nanotube axis as shown in figure (a) and (b) while in figure (c) there is no line of symmetry. Therefore a term C_h which is the vector of helicity is defined mathematically when the graphene sheet is rolled into tubes in the different ways in which the angle of helicity is θ.

$$\boldsymbol{C_h = n\overrightarrow{a_1} + m\overrightarrow{a_2}}$$

$$\boldsymbol{\cos\theta = \frac{2n + m}{2\sqrt{n^2 + m^2 + nm}}}$$

Where $\overrightarrow{a_1}$ and $\overrightarrow{a_2}$ are primitive lattice vector.

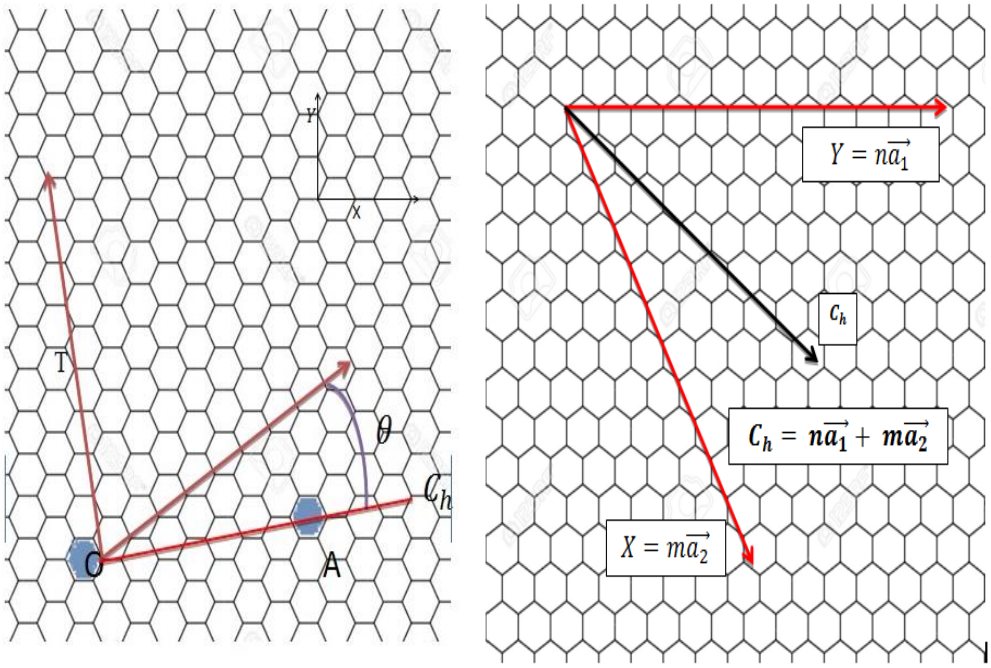

Fig.1.4 Structure of Single Walled Carbon Nanotube

Depending on their chirality or the way of folding, the carbon nanotubes are classified in three ways as Zigzag CNT, Armchair CNT and Helical CNT.

1.4.1 Zigzag CNT

These CNTs are formed for $\theta = 0$ and chirality (n, 0), where n = 0, 1, 2, 3, …… Because of the zig zag arrangement of carbon atoms, these are termed as zig-zag CNTs.

1.4.2 Armchair CNT

These CNTs are formed for $\theta = \pi / 6$ and chirality (n, n).

1.4.3 Helical CNT

These CNTs are formed for the angle which is anywhere in between 0 and $\pi / 6$ and the chirality is (n, m) where n $\neq$ m.

These structures are shown in the figure below

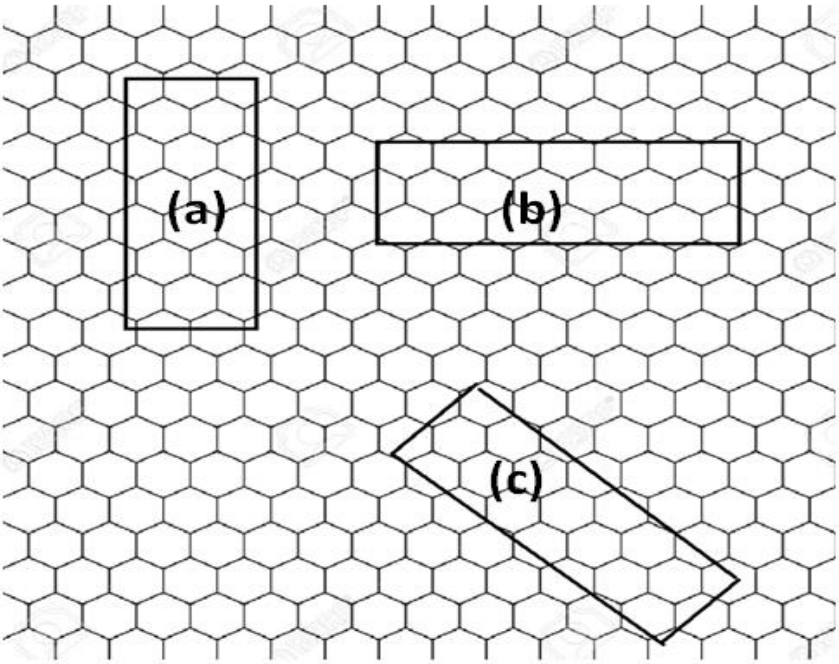

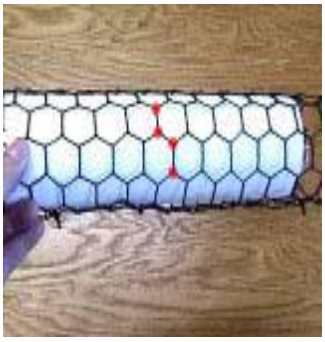

(a)Armchair arrangement of carbon atoms

(b) Zig-zag arrangement of carbon atoms

(c) Chiral arrangement of carbon atoms

Fig. 1.5 Nanotubes Geometry

1.5 Synthesis of CNT

Synthesis of carbon nanotubes can be done by three methods i.e. Arc-discharge method, Laser-ablation method and Catalytic growth. The multi walled carbon nanotubes were first discovered by Arc-discharge method. For the production of carbon fibres and fullerenes, Arc-discharge method has been used. Bundle of aligned single walled carbon nanotubes with

small diameter was synthesized by Laser-ablation method which was a significant progress. Yacaman used the Chemical Vapour Decomposition (CVD) for Catalytic growth of nanotubes. So these are the three techniques of the synthesis of the CNT.

Chapter 2

THEORY OF FIELD EMISSION

2.1 Field Emission

When electrons are extracted from a metal or a semiconducting surface by applying a very high electric field, this process is called field emission. In other words, by applying a very high electric field, the emission of the electrons from a metal or semiconductor into a vacuum or in a dielectric is called the field emission. In this process, electrons tunnel across a potential barrier. This effect is completely analog. It occurs when the wave function of an electron decays exponentially into the barrier (electron's potential energy is greater than electron's total energy) the wave function of electrons does not disappear at the classical turning point. So the electron will found at the outside of the barrier.

Field emission, which is also termed as field electron emission or electron field emission, is the emission of electrons that are induced in the existence an electrostatic field. The field emission can change from solid or liquid surfaces into air or any conducting or non conducting dielectric. When the electrons move from the valance band to conduction band, under the induced field promotion, then this process of semiconductors can also be termed as a field emission of electrons.

In pure metals, for field emission, a very high electric field is required such as the gradients must be higher than 1 G V/m and should be dependent on the work function. Electron sources have a lot of applications when they are based on the field emission. Later, the quantum tunnelling of electrons explained the field emission. This was one of the major success of the quantum mechanics.

For a parallel flat electrode, the field is 10^9 V/m. If the separation between anode and cathode is 1 nm then the voltage will be approximately 1000 KV. The electrons can be emitted at a low applied electric field when the cathode has a very high point. The electrons can tunnel across the energy barrier which is near the Fermi level and under the influence of high electric field, the electrons goes to the vacuum level. The width of potential barrier is reduced when the field is applied to a cathode surface as shown in the figure.

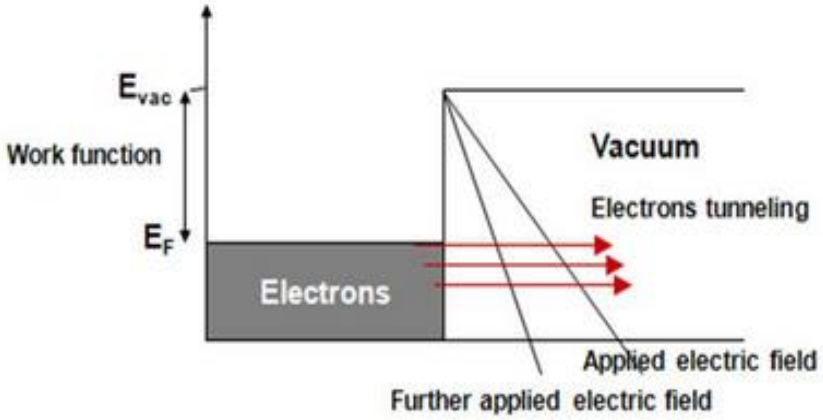

Fig. 2.1 Effect of electric field on the energy barrier for electrons.

By quantum mechanical tunnelling, the carriers can pass through the barrier. The first generally accepted explanation of field emission in terms of quantum mechanics is provided by Fowler-Nordhiem (F-N) which they applied for the electronic energy levels in metal to the sommerfeld model. They defined a relationship between the field emission current density and applied electric field.

The Fowler-Nordhiem (F-N) equation for the field emission current density (J) is given by

$$J = \frac{aE_t^{\,2}}{\phi}\exp\left(\frac{-b\phi^{3/2}}{E_t}\right),$$

where

$a = 1.56\times10^{-6}\ AV^{-2}eV$,

$b = 6.83\times10^{7}\ eV^{-3/2}Vcm^{-1}$,

E_t = Electric field at the tip,

ϕ = work function.

As E_t is written as βE, where E is V/d, is the applied field and the term β is the field enhancement factor and this can be written as h / r, where h is the height of the tip and r is the radius of the curvature. So the J can be rewritten as

$$J = \frac{a(\beta E)^2}{\phi} \exp\left(\frac{-b\phi^{3/2}}{\beta E}\right).$$

As nanotubes produce very high current densities and show low operating voltage so they compare with the other field emission sources.

Chapter 3

FIELD EMISSION OF ELECTRONS FROM HEMISPHERICAL CONDUCTING CNT TIP

3.1 Introduction

Carbon nanotubes have excellent properties which are, having good chemical stability, good mechanical strength, and high thermal conductivity and high aspect ratio. They also have unique electrical properties. So due to these excellent properties, they are being extensively studied. In recent years, the growth mechanism of carbon nanotube is a very important field of research in the plasma environment. Different studies have stated that the carbon nanotubes emit high current densities as 10 mA/cm^2.

As carbon nanotubes have very high values of the current density as compared to the other field emission devices, the field emission properties is then another important area of research. When carbon nanotube is substituted by nitrogen then the field emission properties can be improved, when the substituted tube have a lower work function. The field emission is studied from the patterned CNT films and revealed that the field emission is depend on the density and morphology of the carbon nanotube and a low current is yield by low and high density films due to the screening effects.

By studying the properties of field emission of single walled nanotubes, the current density is obtained and the value of this current density is 10 mA/cm^2. The carbon nanotubes shows very good emission properties when the field emitters are desined by carbon nanotubes and at lower electric field, field emitters emit current densities of 10 mA/cm^2.

The dimension of single wall nanotubes has a great effect on the field emission properties of the carbon nanotubes. When the carbon nanotube is replaced with nitrogen then the field emission properties could be improved because the substituted tube has a very low work function.

The electric field distributed on the top of the surface of the carbon nanotube can be used to determine the field emission from a carbon nanotube. For device application, the emission performance from array of nanotubes is limited by field screening effect. The field emission properties of carbon nanotubes and the role of the extrinsic atoms in the morphology have been studied. The carbon atoms can be replaced by the dopant nitrogen in the multiwall carbon nanotube then the electron density is increased, the effect of this is that the field emission properties are enhanced. The concentration of the electrons and holes are increased when Boron is inserted into the carbon nanotube.

The image method is introduced for solving the field enhancement factor. It is done at the apex. The result of this is that the field enhancement factor is marginally affected by the distance between the cathode and anode and when this distance is decreased, a low threshold voltage is obtained. The anode and the emitter tip make an arrangement of parallel plate when the anode is brought at the emitter tip then the field enhancement factor reaches to unity. The field enhancement factor decreases with the carbon nanotube radius from the multi walled carbon nanotubes.

Carbon nanotubes have good electronic structure, good chemical inertness and a very aspect ratio, so they have excellent field emission properties. The field enhancement factor is affected in a distribution of carbon nanotube by the length of carbon nanotubes and the spacing between them. There are many experiments have been carried out for the field enhancement factor to see the effect of the length of carbon nanotubes and the spacing between them. By using screening effect, Bonard have revealed the expression to calculate the field enhancement factor.

So here we study the potential energy and the field emission current density function of emitted electrons from a hemispherical conducting carbon nanotube tip in the absence of image force. So in the absence of image force, here we develop a theoretical model for the potential and then the potential energy of an emitted electron at a distance r from the centre of a hemispherical carbon nanotube of radius a and having charge q. After that for the solution of the transmission probability of the emitted electrons, we use the time independent Schrodinger equation using the JWKB approximation. After that the field emission current density function ϕ has been derived. Results and discussion part is given in chapter 4.

3.2 MODEL

Consider a conducting CNT with a hemispherical cap of radius a in a vacuum and with the potential energy of an electron of charge q at a distance r from the surface of the spherical C N T .

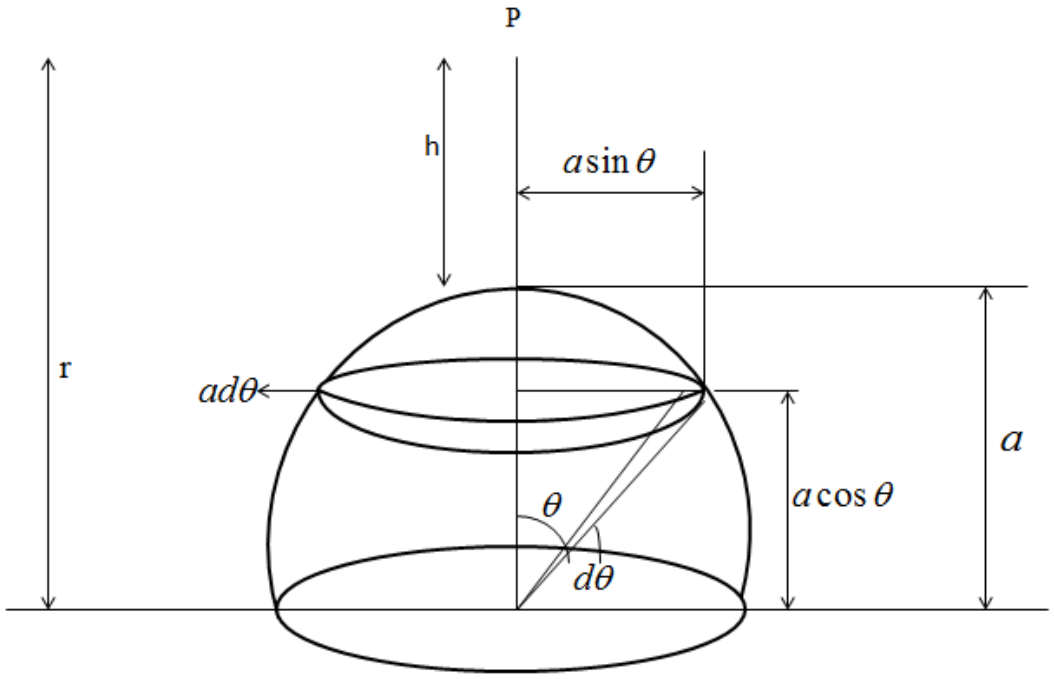

Fig. 3.1 Schematic diagram of Hemispherical CNT tip

Let us consider a ring in this hemisphere of width $ad\theta$. The distance of the point to the centre of the hemisphere is r. By analysing this diagram the distance of the point P to the centre of the small ring will be $(h+a-a\cos\theta)$. If σ is surface charge density then the charge on this ring will be

$$dq = \sigma \times 2\pi a \sin\theta \times ad\theta ,$$

Hence the electric field at point P due to this small ring will be

$$dE = \frac{1}{4\pi\varepsilon_0} \frac{\sigma \times 2\pi a \sin\theta \times ad\theta (h+a-a\cos\theta)}{\{(a^2 \sin^2\theta)+(h+a-a\cos\theta)^2\}^{\frac{3}{2}}} ,$$

$$dE = \frac{1}{4\pi\varepsilon_0} \frac{\sigma \times 2\pi a \sin\theta \times a d\theta (h + a - a\cos\theta)}{\{a^2 \sin^2\theta + h^2 + a^2(1-\cos\theta)^2 + 2ah(1-cos\theta)\}^{\frac{3}{2}}} \ ,$$

$$dE = \frac{\sigma a^2}{2\varepsilon_0} \frac{\sin\theta (h + a - a\cos\theta) d\theta}{\{a^2 \sin^2\theta + h^2 + a^2 + a^2\cos^2\theta - 2a^2\cos\theta + 2ah - 2ah\cos\theta\}^{\frac{3}{2}}} \ ,$$

$$dE = \frac{\sigma a^2}{2\varepsilon_0} \frac{\sin\theta (h + a - a\cos\theta) d\theta}{\{2a^2 + h^2 - 2a^2\cos\theta + 2ah(1-\cos\theta)\}^{\frac{3}{2}}} \ ,$$

$$dE = \frac{\sigma a^2}{2\varepsilon_0} \frac{\sin\theta (h + a - a\cos\theta) d\theta}{h^3 \left\{2\frac{a^2}{h^2} + 1 - 2\frac{a^2}{h^2}\cos\theta + 2\frac{a}{h}(1-\cos\theta)\right\}^{\frac{3}{2}}} \ ,$$

We can put $\frac{a^2}{h^2} = 0$, because radius of carbon nanotube will be in nano meter and distance from top will be in micro meter.

So we can write

$$dE = \frac{\sigma a^2}{2\varepsilon_0} \frac{\sin\theta (h + a - a\cos\theta) d\theta}{h^3 \left\{1 + 2\frac{a}{h}(1-\cos\theta)\right\}^{\frac{3}{2}}} \ ,$$

So the electric field will be

$$E = \frac{\sigma a^2}{2\varepsilon_0 h^3} \int_0^{\pi/2} \frac{\sin\theta (h + a - a\cos\theta) d\theta}{\left\{1 + 2\frac{a}{h}(1-\cos\theta)\right\}^{\frac{3}{2}}} \ ,$$

Calculating this integral we find the electric field

$$E = \frac{\sigma a^2}{2\varepsilon_0 h^2} \frac{1}{\sqrt{1+\frac{2a}{h}}} \ .$$

Now we have to find out the potential at hemispherical CNT tip at distance r. So from basics of potential of charged ring we know that the potential at any point on the axis of a ring is

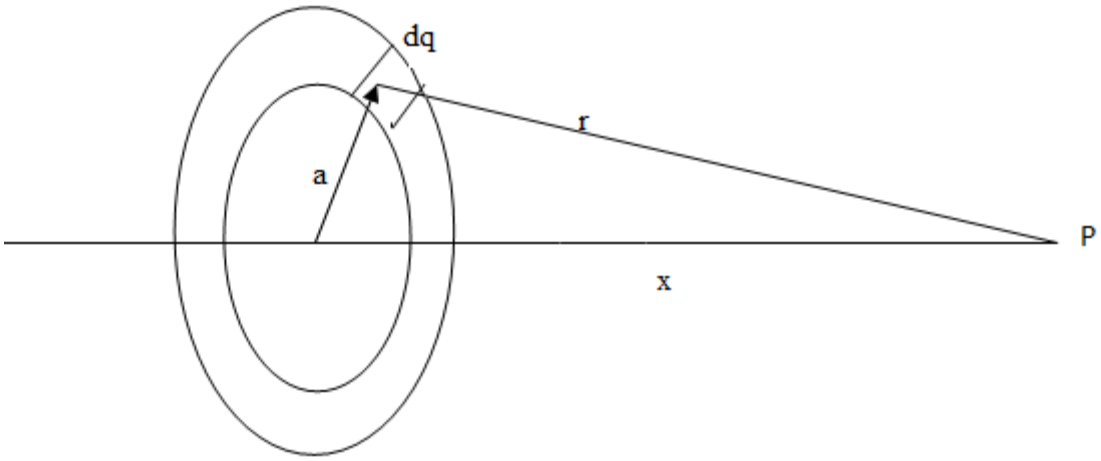

Fig. 3.2 Electric Potential of charged ring

$$V = \frac{kQ}{\sqrt{x^2 + a^2}}, \qquad \text{where } k = \frac{1}{4\pi\varepsilon_0}.$$

where Q is total charge on the ring, x is the distance from the centre of ring to the point at which we are calculating the potential, and a is the radius of the ring.

So by applying this concept in our problem, we can find out the potential of hemispherical CNT tip at distance r from the surface of the tip.

$$dV = \frac{2\pi a \sin\theta \times \sigma \times a d\theta}{4\pi\varepsilon_0 \left\{(a\sin\theta)^2 + (h + a - a\cos\theta)^2\right\}^{\frac{1}{2}}},$$

$$dV = \frac{2\pi a^2 \sigma \sin\theta d\theta}{4\pi\varepsilon_0 \left\{a^2 \sin^2\theta + h^2 + (a - a\cos\theta)^2 + 2h(a - a\cos\theta)\right\}^{\frac{1}{2}}} ,$$

$$dV = \frac{2\pi a^2 \sigma \sin\theta d\theta}{4\pi\varepsilon_0 \left\{a^2 \sin^2\theta + h^2 + a^2 + a^2\cos^2\theta - 2a^2\cos\theta + 2ha(1-\cos\theta)\right\}^{\frac{1}{2}}} ,$$

$$dV = \frac{2\pi a^2 \sigma \sin\theta d\theta}{4\pi\varepsilon_0 \left\{h^2 + 2a^2 - 2a^2\cos\theta + 2ha(1-\cos\theta)\right\}^{\frac{1}{2}}} ,$$

$$dV = \frac{a^2 \sigma \sin\theta d\theta}{2\varepsilon_0 h\left\{1 + 2\frac{a^2}{h^2} - 2\frac{a^2}{h^2}\cos\theta + 2\frac{a}{h}(1-\cos\theta)\right\}^{\frac{1}{2}}} , \qquad (a)$$

We can put $\frac{a}{h} = 0$, because radius of carbon nanotube will be in nano meter and distance from top will be in micro meter.

So we can write

$$dV = \frac{a^2 \sigma \sin\theta d\theta}{2\varepsilon_0 h} ,$$

So

$$V = \frac{a^2 \sigma}{2\varepsilon_0 h}\int_0^{\pi/2} \sin\theta d\theta ,$$

$$V = \frac{a^2 \sigma}{2\varepsilon_0 r} .$$

So this is the potential of hemispherical CNT tip at distance r from the surface of the tip but for more accurate potential we can put $\frac{a^2}{h^2} = 0$ instead of $\frac{a}{h} = 0$ so from equation (a) we have

$$dV = \frac{a^2\sigma \sin\theta d\theta}{2\varepsilon_0 h\left\{1+2\frac{a}{h}(1-\cos\theta)\right\}^{\frac{1}{2}}},$$

So

$$V = \frac{a^2\sigma}{2\varepsilon_0 h}\int_0^{\pi/2} \frac{\sin\theta d\theta}{\left(1+\frac{2a}{h}(1-\cos\theta)\right)^{\frac{1}{2}}},$$

$$V = \frac{a^2\sigma}{2\varepsilon_0 h}\int_0^{\pi/2} \sin\theta\left\{1+\frac{2a}{h}(1-\cos\theta)\right\}^{-\frac{1}{2}} d\theta,$$

By applying binomial theorem

$$V = \frac{a^2\sigma}{2\varepsilon_0 h}\int_0^{\pi/2} \sin\theta\left\{1-\frac{1}{2}\frac{2a}{h}(1-\cos\theta)\right\} d\theta,$$

$$V = \frac{a^2\sigma}{2\varepsilon_0 h}\int_0^{\pi/2} \sin\theta\left\{1-\frac{a}{h}(1-\cos\theta)\right\} d\theta,$$

Let $1-\cos\theta = x$,

$\sin\theta d\theta = dx$,

Limit $\theta = 0 \rightarrow x = 0$,

$\theta = \pi/2 \rightarrow x = 1$,

$$V = \frac{a^2\sigma}{2\varepsilon_0 h}\int_0^1 (1-\frac{a}{h}x)dx,$$

$$V = \frac{a^2\sigma}{2\varepsilon_0 h}\left[1-\frac{a}{2h}\right].$$

So this is the potential of hemispherical CNT tip at distance h from the surface of the tip.

Now $\sigma = \frac{q}{2\pi a^2}$,

So

$$V = \frac{q}{4\pi\varepsilon_0 h}\left[1 - \frac{a}{2h}\right].$$

The potential energy is

$$V(h) = \frac{q^2}{4\pi\varepsilon_0 h}\left[1 - \frac{a}{2h}\right].$$

Normalizing this equation as let $r = h + a$,

$$V(r) = \frac{q^2}{4\pi\varepsilon_0 (r-a)}\left[1 - \frac{a}{2(r-a)}\right] \quad . \tag{1}$$

So the plot for variation of the potential energy V(r) with respect to the radial distance r is shown below

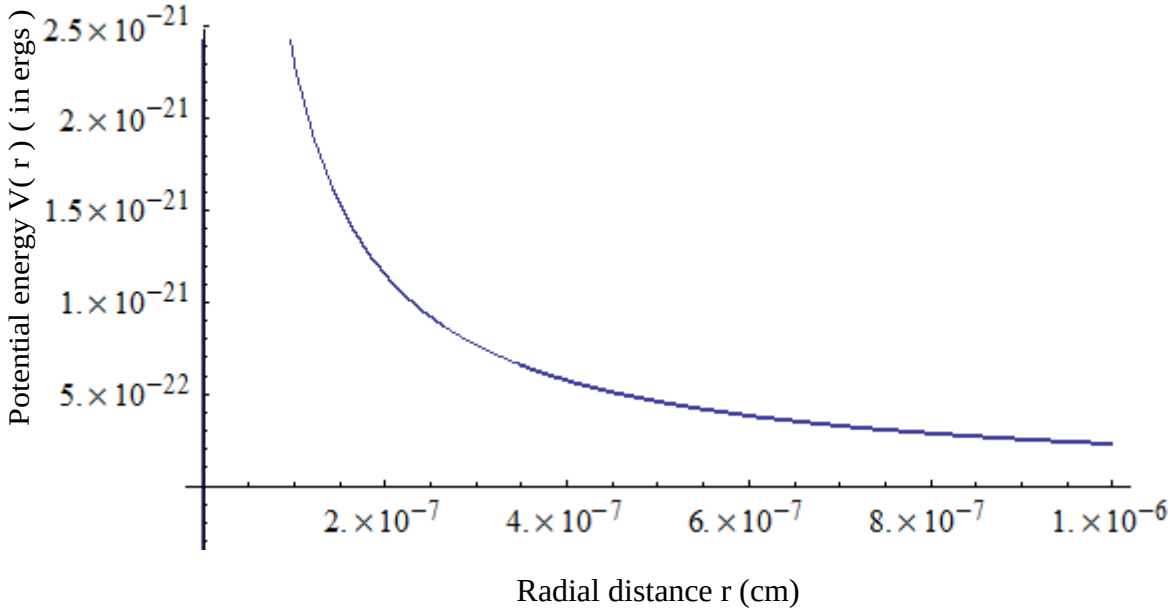

Fig. 3.3 Variation of the potential energy w.r. t. the radial distance

Let us consider the time-independent Schrodinger wave equation. The time-independent Schrodinger wave equation for the region $r > a$ is given by

$$\nabla^2\psi(r,\theta,\phi)+\frac{2m_e}{\hbar^2}\left[E-\frac{q^2}{4\pi\varepsilon_0(r-a)}\left(1-\frac{a}{2(r-a)}\right)\right]\psi(r,\theta,\phi)=0, \qquad \text{for r > a} \qquad (2)$$

where $\hbar$ is $h/2\pi$, h is the Planck's constant, m_e is the mass of the electron, and $\psi(r,\theta,\phi)$ is the wave function of electrons which is emitted from the conducting carbon nanotube. Now to separate the radial and angular term of this Schrodinger equation, we use the separation of variable method. So we can write

$$\psi(r,\theta,\phi)=R(r)Y(\theta,\phi)=\frac{U(r)}{r}Y(\theta,\phi), \qquad (3)$$

from equation (2) and (3), we can write

$$\frac{d^2U(r)}{dr^2}+\frac{2m_e}{\hbar^2}\left[E-\frac{q^2}{4\pi\varepsilon_0(r-a)}\left(1-\frac{a}{2(r-a)}\right)-\frac{\hbar^2}{2m_e r^2}l(l+1)\right]U(r)=0, \qquad \text{for r > a} \qquad (4)$$

where l is the angular momentum quantum number of the electron, and the term $\frac{\hbar^2}{2m_e r^2}l(l+1)$ is the angular energy.

Substituting

$$E-\frac{\hbar^2}{2m_e r^2}l(l+1)=E_r, \qquad (5)$$

where E_r is the radial energy, (4) can be rewritten as

$$\frac{d^2U(r)}{dr^2}+\frac{2m_e}{\hbar^2}\left[E_r-\frac{q^2}{4\pi\varepsilon_0(r-a)}\left(1-\frac{a}{2(r-a)}\right)\right]U(r)=0, \qquad \text{for r > a} \qquad (6)$$

Now we can normalize the above equation using $\rho = r/a$ for $r > a$, we have

$$\frac{d^2U(\rho)}{d\rho^2}+\frac{2m_eV_0a^2}{\hbar^2}\left[\frac{E_\rho}{V_0}-\frac{q^2}{4\pi\varepsilon_0V_0(a\rho-a)}\left(1-\frac{a}{2(a\rho-a)}\right)\right]U(\rho)=0, \tag{7}$$

$$\frac{d^2U(\rho)}{d\rho^2}+\frac{2m_eV_0a^2}{\hbar^2}\left[\frac{E_\rho}{V_0}-\frac{q^2}{4\pi\varepsilon_0V_0a(\rho-1)}\left(1-\frac{1}{2(\rho-1)}\right)\right]U(\rho)=0, \tag{8}$$

$$\frac{2m_eV_0a^2}{\hbar^2}=\beta, \tag{9}$$

$$\frac{E_\rho}{V_0}=\varepsilon_\rho, \tag{10}$$

$$\frac{q^2}{4\pi\varepsilon_0V_0a}=\eta, \tag{11}$$

And

$$\frac{d^2U(\rho)}{d\rho^2}+\Gamma^2U(\rho)=0, \tag{12}$$

Here Γ is given by

$$\Gamma^2=\beta\left(\varepsilon_\rho-\frac{\eta}{(\rho-1)}\left(1-\frac{1}{2(\rho-1)}\right)\right).$$

3.3 Electron transmission coefficient

The probability of electronic tunnelling $T(\varepsilon_\rho)$, from the hemispherical conducting carbon nanotube tip and using the JWKB approximation, can be given as

$$T(\varepsilon_\rho)=\exp\left(-2\int_{\rho_1}^{\rho_2}\sqrt{-\Gamma^2}\,d\rho\right) \qquad \text{for r > a} \tag{13}$$

Now we have to find out the probability of electronic tunnelling for which we need the values of β and η for different radius of carbon nanotube. So here is the calculation:

$$\beta = \frac{2m_e V_0 a^2}{\hbar^2},$$

In CGS unit $m_e = 9.1\times10^{-28}\, gm,$

$V_0 = 5 \text{ eV} = 5\times1.6\times10^{-12} \text{ erg},$

$\hbar = 1.05\times10^{-27}\ erg-\text{sec}.$

For a = 0.5 nm

$\beta = 32.765,$

$\eta = 0.576,$

For a = 1 nm

$\beta = 131.0625,$

$\eta = 0.288,$

For a = 1.5 nm

$\beta = 297.14,$

$\eta = 0.192,$

For a = 2 nm

$\beta = 524.25,$

$\eta = 0.144,$

So now calculating the Transmission coefficient, $T(\varepsilon_\rho)$ as a function of normalized radial energy, ε_ρ at the tip of the carbon nanotube, at the radius of the hemispherical conducting CNT (i.e., a = 0.5 nm):

For a = 0.5 nm

The Transmission coefficient, $T(\varepsilon_\rho)$ is defined by

$$T(\varepsilon_\rho) = \exp\left(-2\int_{\rho_1}^{\rho_2} \sqrt{-\Gamma^2}\, d\rho \right),$$

where

$$\Gamma^2 = \beta\left(\varepsilon_\rho - \frac{\eta}{(\rho-1)}\left(1 - \frac{1}{2(\rho-1)}\right)\right).$$

So we are calculating the integral using MATHEMATICA software taking values of radial energy from 0.01 to 0.035 at regular intervals of 0.005.

For a = 0.5 nm

$\beta = 32.765$,

$\eta = 0.576$,

At different radial energies, corresponding transmission coefficients are given in the table below

Radial Energy (ε_ρ)	**Transmission Coefficient $T(\varepsilon_\rho)$**
0.010	0.0660
0.015	0.0681
0.020	0.0702
0.025	0.0724
0.030	0.0747
0.035	0.0771

Table 3.1 Radial energy w.r.t. Transmission coefficient for 0.5 nm

So the transmission probability, $T(\varepsilon_\rho)$ variation with the normalized radial energy, ε_ρ at the hemispherical conducting CNT tip at the radius 0.5 nm is shown below

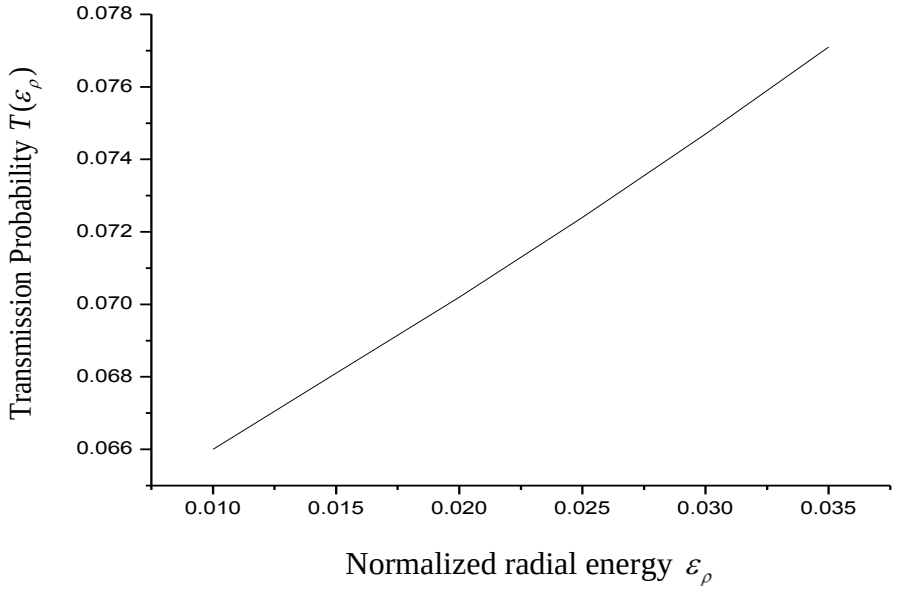

Fig. 3.4 Variation of transmission coefficient with normalized radial energy of radius 0.5 nm

For a = 1 nm

Calculating the integral of Transmission coefficient using MATHEMATICA software taking values of radial energy from 0.01 to 0.035 .

$\beta = 131.0625$,

$\eta = 0.288$,

At different radial energies, corresponding transmission coefficients are given in the table below

Radial Energy (ε_ρ)	**Transmission Coefficient $T(\varepsilon_\rho)$**
0.010	0.0233
0.015	0.0255
0.020	0.0279
0.025	0.0306
0.030	0.0337
0.035	0.0372

Table 3.2 Radial energy w.r.t. Transmission coefficient for 1 nm

So the transmission probability, $T(\varepsilon_\rho)$ variation with the normalized radial energy, ε_ρ at the hemispherical conducting CNT tip at the radius 1 nm is shown below

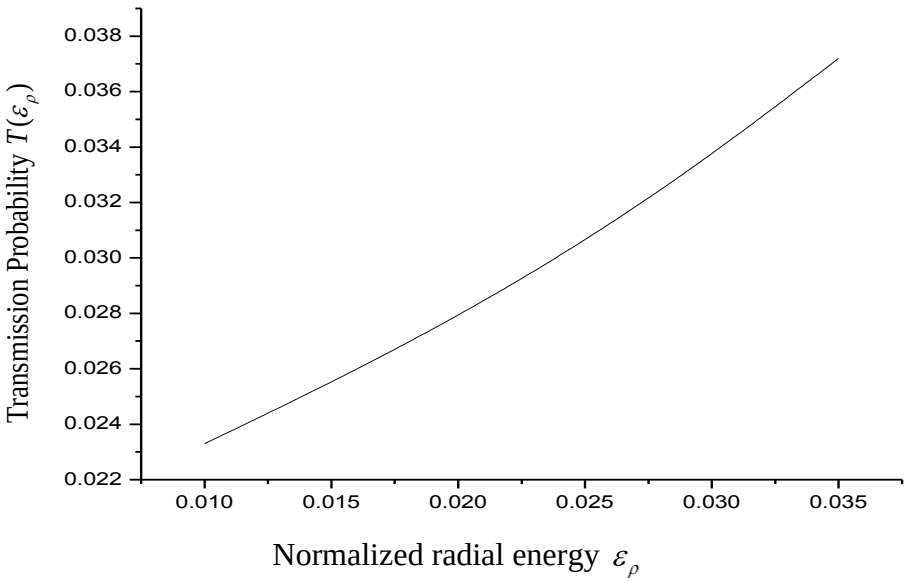

Fig. 3.5 Variation of transmission coefficient with normalized radial energy of radius 1 nm

<u>For a = 1.5 nm</u>

Calculating the integral of Transmission coefficient using MATHEMATICA software taking values of radial energy from 0.01 to 0.035.

$\beta = 297.14$,

$\eta = 0.192$,

At different radial energies, corresponding transmission coefficients are given in the table below

Radial Energy (ε_ρ)	**Transmission Coefficient $T(\varepsilon_\rho)$**
0.010	0.0110
0.015	0.0130
0.020	0.0155
0.025	0.0186
0.030	0.0225
0.035	0.0275

Table 3.3 Radial energy w.r.t. Transmission coefficient for 1.5 nm

So the transmission probability, $T(\varepsilon_\rho)$ variation with the normalized radial energy, ε_ρ at the hemispherical conducting CNT tip at the radius 1.5 nm is shown below

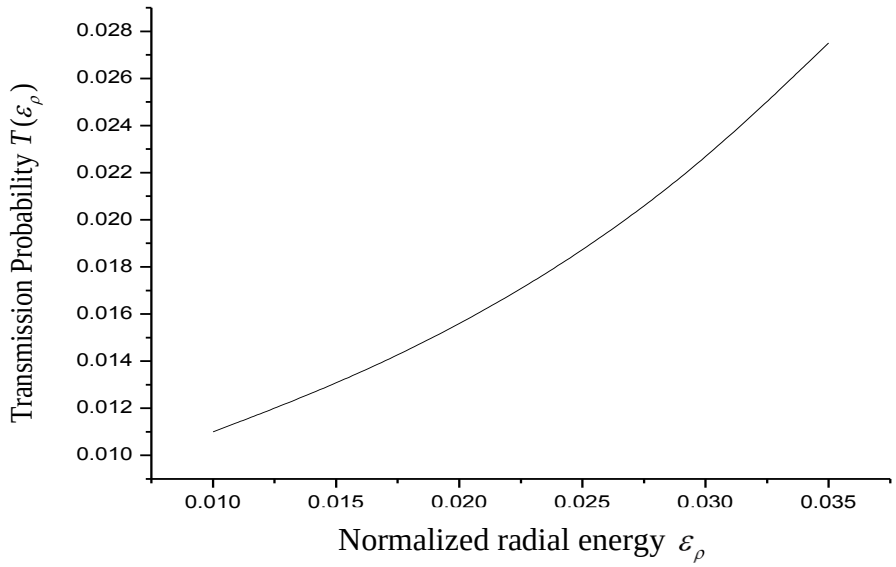

Fig. 3.6 Variation of transmission coefficient with normalized radial energy of radius 1.5 nm

For a = 2 nm

Calculating the integral of Transmission coefficient using MATHEMATICA software taking values of radial energy from 0.01 to 0.035.

$\beta = 524.25$,

$\eta = 0.144$,

At different radial energies, corresponding transmission coefficients are given in the table below

Radial Energy (ε_ρ)	**Transmission Coefficient $T(\varepsilon_\rho)$**
0.010	0.00635
0.015	0.00829
0.020	0.0109
0.025	0.0148
0.030	0.0205
0.035	0.0263

Table 3.4 Radial energy w.r.t. Transmission coefficient for 2 nm

So the transmission probability, $T(\varepsilon_\rho)$ variation with the normalized radial energy, ε_ρ at the hemispherical conducting CNT tip at the radius 2 nm is shown in the graph.

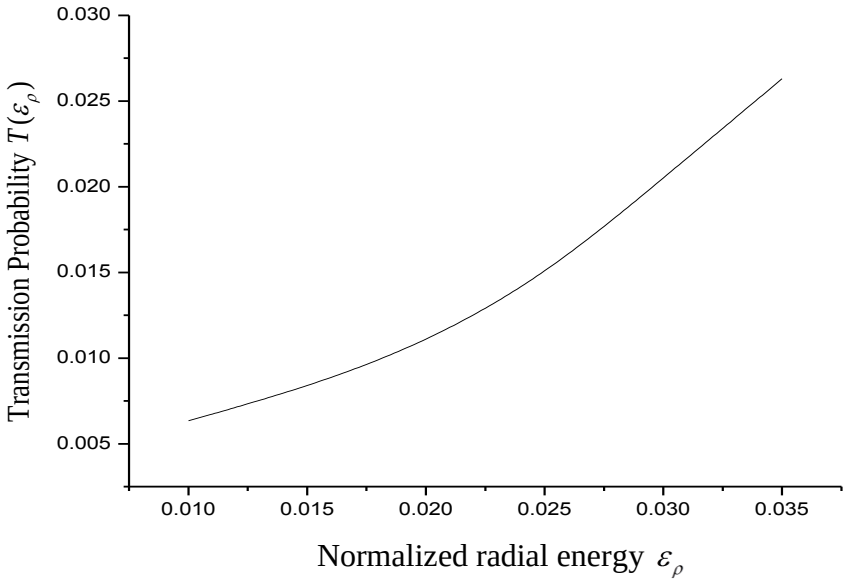

Fig. 3.7 Variation of transmission coefficient with normalized radial energy of radius 2 nm

3.4 Field Emission Current Density

When the temperature of the cathode is 0 K, then the emitted electrons from the cathode produces a current, which is known as field emission current density. So the field emission current density is given by

$$J\left(\varepsilon_\rho, \varepsilon_f, T(\varepsilon_\rho)\right) = \frac{4\pi m_e e}{\hbar^3} V_0^{\,2} \int_0^{\varepsilon_f} (\varepsilon_f - \varepsilon_\rho) T(\varepsilon_\rho) d\varepsilon_\rho .$$

Here the current density J is the function of the radial energy ε_ρ, Fermi energy, ε_f and the transmission coefficient. The current density function ϕ is given as

$$\phi = \int_0^{\varepsilon_f} (\varepsilon_f - \varepsilon_\rho) T(\varepsilon_\rho) d\varepsilon_\rho .$$

The value of coefficients are

$m_e = 9.1\times10^{-28}$ gm,

$e = 4.8\times10^{-10}$ esu,

$V_0 = 5$ eV $= 5\times1.6\times10^{-12}$ erg,

$\hbar = 1.05\times10^{-27}$ erg-sec.,

$$\frac{4\pi m_e e}{\hbar^3} V_0^{\,2} = 3.03\times10^{23}.$$

Now we are calculating the current density function for different radius.

For a = 0.5 nm

The fourth order polynomial of transmission coefficient for calculating current density function from software origin 8 is

$T(\varepsilon_\rho) = \text{intercept} + B_1 x + B_2 x^2 + B_3 x^3 + B_4 x^4$,

So for a = 0.5 nm

Intercept = 0.06127,

B_1 = 0.54693,

B_2 = -10.41667,

B_3 = 337.03704,

B_4 = -3333.33333,

Hence the current density function is

$$\phi_1 = \int_{0.01}^{0.035} (y - x) * (0.06127 + 0.54693x - 10.41667x^2 + 337.037x^3 - 3333.3333x^4)\, dx$$

$$= -0.0000407297 + 0.00178465y$$

where y is the Fermi energy and x is the radial energy.

The variation of the current density function ϕ, with respect to the normalized Fermi energy, ε_f at the hemispherical conducting CNT tip at the radius 0.5 nm is shown below

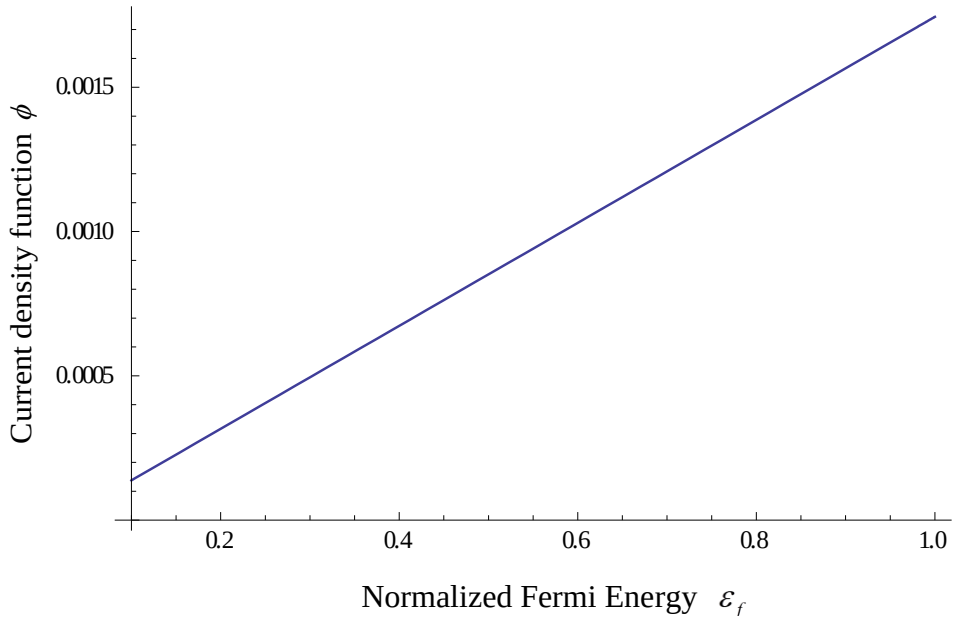

Fig. 3.8 Variation of current density function with normalized Fermi energy at radius 0.5 nm

For a = 1 nm

Intercept = 0.01873,

B_1 = 0.51474,

B_2 = -9.41667,

B_3 = 396.2963,

B_4 = -3333.33333,

Hence the current density function is

$$\phi_2 = \int_{0.01}^{0.035} (y - x) * (0.01873 + 0.51474x - 9.4166x^2 + 396.2963x^3 - 3333.33333x^4)\, dx$$

$$= -0.0000173456 + 0.000739086y$$

The variation of the current density function ϕ, with respect to the normalized Fermi energy, ε_f at the hemispherical conducting CNT tip at the radius 1 nm is shown below

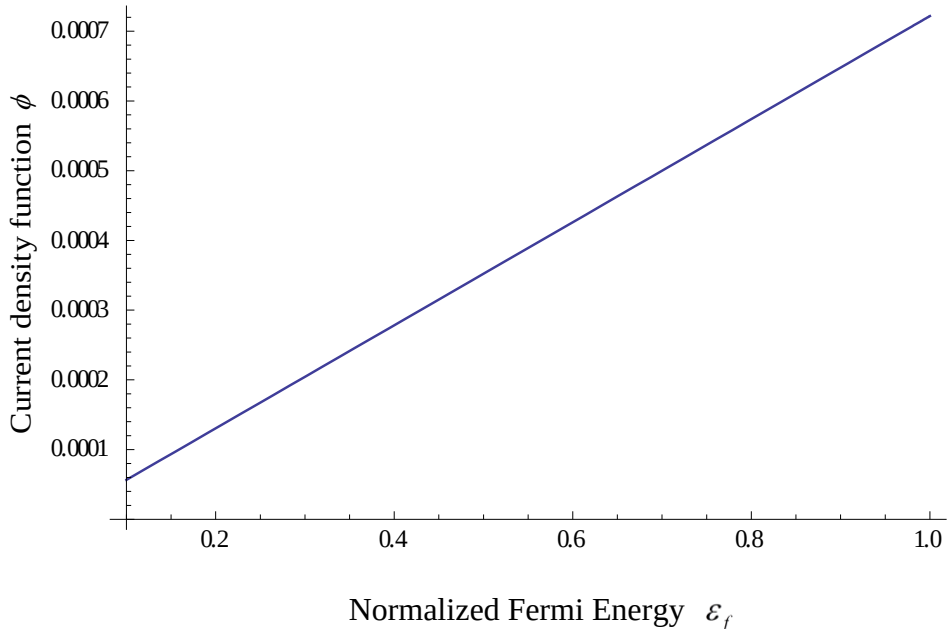

Fig. 3.9 Variation of current density function with normalized Fermi energy at radius 1 nm

For a = 1.5 nm

Intercept = 0.0086,

B_1 = 0.10833,

B_2 = 15.83333,

B_3 = -333.33333,

B_4 = 6666.66667,

Hence the current density function is

$$\phi_3 = \int_{0.01}^{0.035} (y - x) * (0.0086 + 0.10833x + 15.8333x^2 - 333.33333x^3 + 6666.66667x^4)\, dx$$

= -0.0000107966 + 0.000442619 y

The variation of the current density function ϕ, with respect to the normalized Fermi energy, ε_f at the hemispherical conducting CNT tip at the radius 1.5 nm is shown below

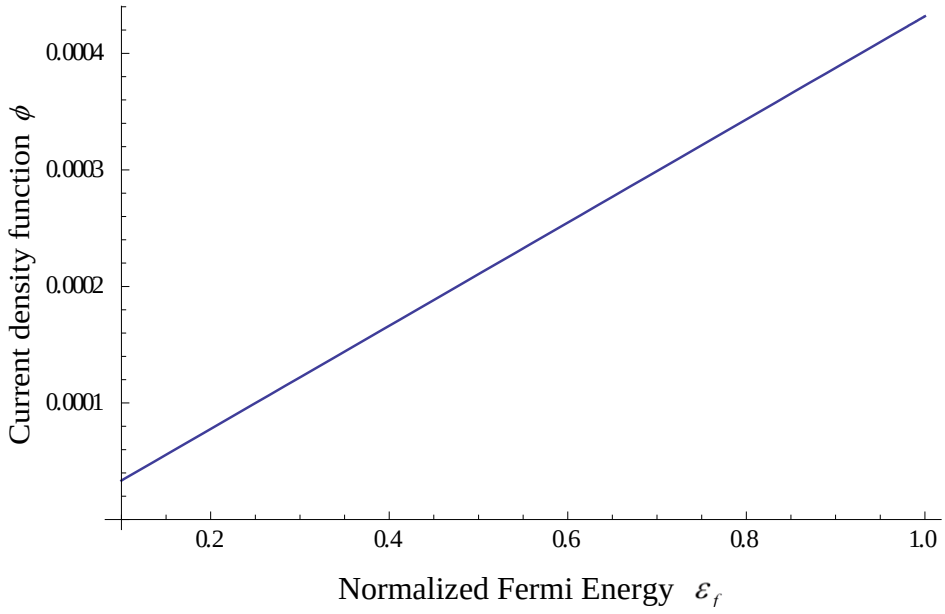

Fig. 3.10 Variation of current density function with normalized Fermi energy at radius 1.5 nm

For a = 2 nm

Intercept = -0.0063,

B_1 = 2.58094,

B_2 = -192.56667,

B_3 = 6862.2222,

B_4 = -77333.3333,

Hence the current density function is

$$\phi_4 = \int_{0.01}^{0.035} (y - x) * (-0.0063 + 2.58x - 192.56667x^2 + 6862.2222x^3 - 77333.33333x^4)\, dx$$

= -0.000008973 + 0.000352299 y

The variation of the current density function ϕ, with respect to the normalized Fermi energy, ε_f at the hemispherical conducting CNT tip at the radius 2 nm is shown below

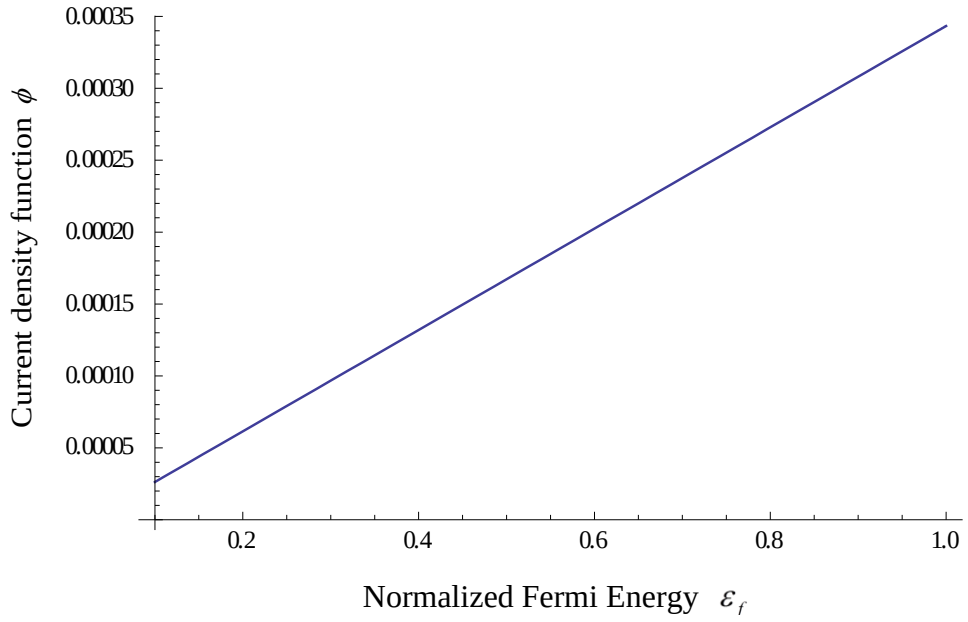

Fig. 3.11 Variation of current density function with normalized Fermi energy at radius 2 nm

Chapter 4

RESULTS

4.1 Results

We have used a number of the CNT parameters to find out the potential, potential energy, transmission coefficient and the field emission current density function. Figure shows the variation of potential of an emitted electron with the radial distance from the hemispherical conducting CNT tip for $r > a$, where r is the distance of point at which the potential is calculated to the centre of hemispherical CNT tip and a is the radius of the CNT. From figure 3.3 we can say that the potential energy decreases with the radial distance, which is the actual behaviour of the potential energy of charged particles.

From equations we have plotted the figures of the transmission coefficient of electrons from the hemispherical conducting CNT tip with the normalized radial energy for the different radius of the hemispherical CNT tip as a = 2, 1.5, 1, 0.5 nm. Graphs illustrates that the electron transmission probability increases with the normalized radial energy. The graph (Fig. 4.1) also illustrates that the transmission coefficient decreases as the radius of the hemispherical conducting CNT tip is increased.

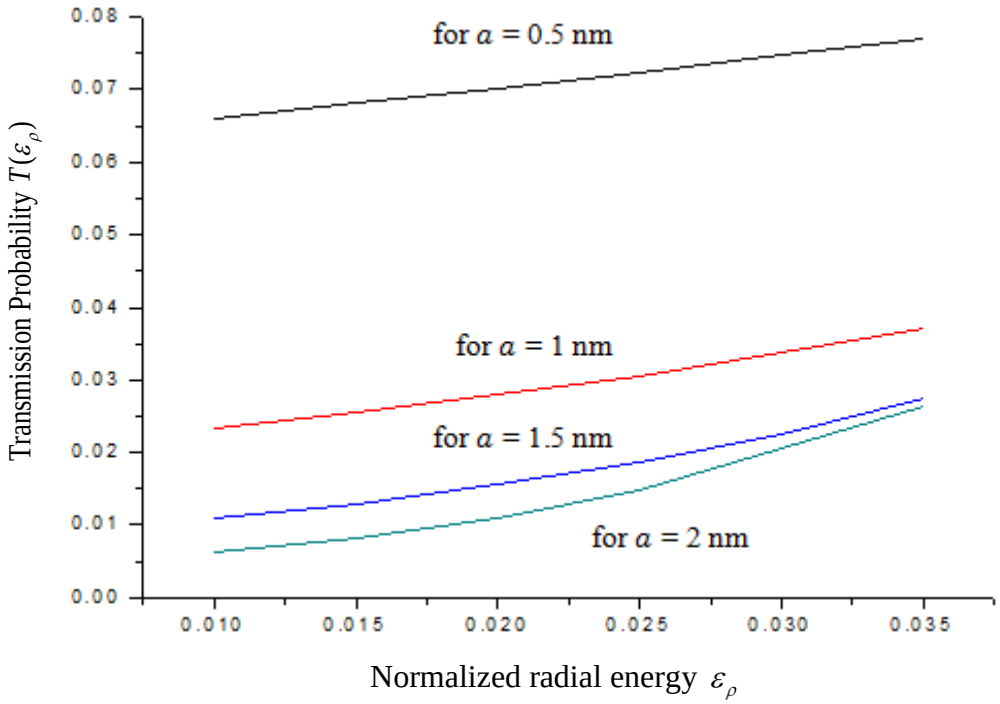

Fig. 4.1 Comparison of all four transmission probabilities

Using equations we plot the graphs of current density function with the normalized Fermi energy by varying the radius of the hemispherical CNT tip such as a = 2, 1.5, 1, 0.5 nm. By observing these figures we can illustrates that the field emission current density function increases with the normalized Fermi energy and also when we increases the hemispherical CNT radius, the field emission current density decreases which is shown in Fig. 4.2.

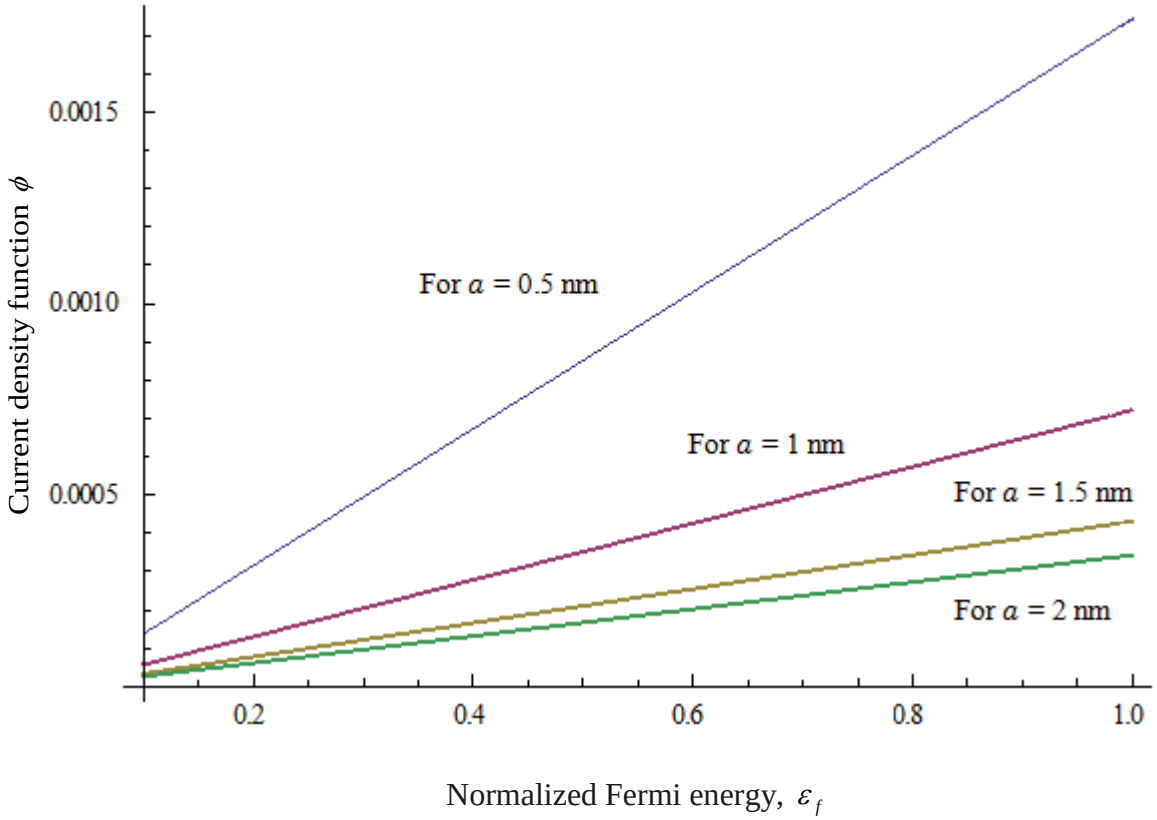

Fig. 4.2 Comparison of all four current density functions

Chapter 5

CONCLUSION

5.1 Conclusion

The conclusion of this model is that the transmission coefficient and the field emission current density function of emitted electrons from the hemispherical CNT tip increases with the normalized radial energy and Fermi energy respectively. The other observation is that when the radius of the hemispherical CNT tip is increased then both the transmission coefficient and field emission current density decreases.

REFERENCE

[1] S. C. Sharma and A. Tewari, Can. J. Phys. **89,** 875 (2011).

[2] P. K. Dubey, J. Phys. D: J. Appl. Phys. **3**, 145 (1970).

[3] M. S. Sodha, A. Dixit, and S. K. Agarwal, Can. J. Phys. **87**, 175 (2009).

[4] J. M. Bonard, J. P. Salvetat, T. Stockli, W. A. de Heer, L. Forró, and A. Châtelain. Appl Phys. Lett. **73**, 918 (1998).

[5] W. Zhu, C. Bower, O. Zhou, G. Kochanski, and S. Jin. Appl. Phys. Lett. **75**, 873 (1999).

[6] D. Y. Zhong, G. Y. Zhang, S. Liu, T. Sakurai, and E. G. Wang, Appl. Phys. Lett. **80**, 506 (2002).

[7] L. Nilsson, O. Groening, C. Emmenegger, O. Kuettel, E. Schaller, L. Schlapbach, H. Kind, J.-M. Bonard, and K. Kern, Appl. Phys. Lett. **76**, 2071 (2000).

[8] L. H. Chan, K. H. Hong, D. Q. Xiao, W. J. Hsieh, S. H. Lai, H. C. Shih, T. C. Lin, F. S. Shieu, K. J. Chen, and H. C. Cheng, Appl. Phys. Lett. **82**, 4334 (2003).

[9] X. Q. Wang, M. Wang, P. M. He, Y. B. Xu, and Z. H. Li, J. Appl. Phys. **96**, 6752 (2004).

[10] R. C. Smith, J. D. Carey, R. D. Forrest, and S.R.P. Silva, J. Vac. Sci. Technol. B, **23**, 632 (2005).

[11] A. Ahmad and V. K. Tripathi, Nanotechnology, **17**, 3798 (2006).

[12] G. Zhang, W. Duan, and B. Gu, Appl. Phys. Lett. **80**, 2589 (2002).

[13] G. Zhou, W. Duan, and B. Gu, Appl. Phys. Lett. **79**, 836 (2001).

[14] J. Luo, L. M. Peng, Z.Q. Xue, and J. L. Wu, Phys. Rev. **66**, 155407 (2002).

[15] S. Han and J. Ihm, Phys. Rev. B, **61**, 9986 (2000).

[16] Y. H. Lee, C. H. Choi, Y. T. Jang, E. K. Kim, B. K. Ju, N. K. Min, and J. H. Ahn, Appl. Phys. Lett. **81**, 745 (2002).

[17] J. S. Suh, K.S. Jeong, J.S. Lee, and I. Han, Appl. Phys. Lett. **80**, 2392 (2002).

[18] J. M. Bonard, C. Klinke, K. Dean, and B. Coll, Phys. Rev. B, **67**, 115406 (2003).

[19] S. H. Jo, Y. Tu, Z.P. Huang, D. L. Carnahan, D. Z. Wang, and Z. F. Ren, Appl. Phys. Lett. **82**, 3520 (2003).

[20] R. C. Che, L. M. Peng, and M. S. Wang, Appl. Phys. Lett. **85**, 4753 (2004).

[21] S. K. Srivastava, A. K. Shukla, V. D. Vankar, and V. Kumar. Thin Solid Films, **492**, 124 (2005).

[22] S. K. Srivastava V. D. Vankar, D. V. Sridhar Rao, and V. Kumar, Thin Solid Films, **515**, 1851 (2006).

[23] S. K. Srivastava, V. D. Vankar, and V. Kumar, Nanoscale Res. Lett. **3**, 25 (2008).

[24] X. Ma and E. G. Wang, Appl. Phys. Lett. **78**, 978 (2001).doi:10.1063/1.1348319.

[25] J. Y. Lee and B. S. Lee, Thin Solid Films, **418**, 85 (2002).

[26] T. Kato, G. H. Jeong, T. Hirata, R. Hatakeyama, K. Tohji, and K. Motomiya, Chem. Phys. Lett. **381**, 422 (2003).

[27] M. S. Sodha and S. Sharma, Br. J. Appl. Phys. **18**, 1127 (1967).

[28] F. Seitz, Modern Theory of Solids. McGraw-Hill, New York.1940.

[29] Z. Xu, X. D. Bai, and E.G. Wang, Appl. Phys. Lett. **88**, 133107 (2006).

[30] R. Gomer, Field Emission and Field Ionization. American Institute of Physics, (New York. 1993. pp. 6–10).

[31] R. H. Fowler and L.W. Nordheim, Proc. R. Soc. Lond. A119, 173 (1928).